Frontiers in Bioscience Landmark

Front. Biosci. (Landmark Ed) **2024**; 29(4): 144
https://doi.org/10.31083/j.fbl2904144

Original Research

UBA2 as a Prognostic Biomarker and Potential Therapeutic Target in Glioma

Yuhong Ou[1,2,†], Hongtao Luo[2,3,†], Qiuning Zhang[2,3], Tianqi Du[1,2], Ruifeng Liu[2,3], Dandan Wang[1,2], Junru Chen[1,2], Meng Dong[1,2], Yuhang Wang[1,2], Zhen Yang[2,4], Xiaohu Wang[1,2,3,*]

[1]The First School of Clinical Medicine, Lanzhou University, 730030 Lanzhou, Gansu, China
[2]Institute of Modern Physics, Chinese Academy of Sciences, 730030 Lanzhou, Gansu, China
[3]Department of Postgraduate, University of Chinese Academy of Sciences, 100043 Beijing, China
[4]School of Public Health, Gansu University of Chinese Medicine, 730030 Lanzhou, Gansu, China
*Correspondence: xhwanggansu@163.com (Xiaohu Wang)
[†]These authors contributed equally.

Academic Editor: Sukmook Lee
Submitted: 6 November 2023 Revised: 8 January 2024 Accepted: 19 January 2024 Published: 9 April 2024

Abstract

Background: Gliomas are characterized by aggressive behavior, leading to severe disability and high mortality. Ubiquitin-like modifier activating enzyme 2 (UBA2) is a subunit of the E1-activating enzyme involved in the SUMOylation (SUMO, small ubiquitin-related modifier) of numerous proteins. Although the abnormality of *UBA2* is linked to the progression of various tumor types, the role of *UBA2* in glioma is still unknown. **Methods**: A bioinformatic analysis using several public databases was conducted to examine the expression level, clinicopathological correlations, and prognostic significance of UBA2 in glioma. The correlation between UBA2 expression and drug sensitivity in cancers was also explored. Multiple cellular experiments were conducted to validate the role of *UBA2* in glioma. **Results**: Analysis of multiple databases and cellular experiments revealed that UBA2 was overexpressed in glioma tissues and cell lines, respectively. UBA2 expression in gliomas correlated with World Health Organization (WHO) grade, *IDH* gene status, *1p19q* deletion, histological type, and immune cell infiltration in glioma. UBA2 expression in carcinomas also correlated with drug sensitivity. Kaplan-Meier analysis revealed that high expression of UBA2 predicted poorer survival in glioma patients. A nomogram model containing UBA2 expression was constructed for clinical practice. Knockdown of *UBA2* was observed to suppress glioma cell progression and sensitize glioma cells to irradiation *in vitro*. **Conclusion**: Overall, this research showed that *UBA2* might be involved not only in the development of glioma but also in the regulation of immunity, drug sensitivity, and radiosensitivity. Therefore, *UBA2* may be a potential target for therapy and a candidate biomarker for glioma diagnosis and prognosis.

Keywords: UBA2; glioma; prognosis; tumor progression; immunity; radiosensitivity

1. Introduction

Gliomas are the most frequent primary intracranial tumors and are characterized by aggressive behavior, leading to severe disability and a high rate of mortality [1]. They are typically classified into two subgroups: low-grade glioma (LGG; grade 2 and 3) and glioblastoma multiforme (GBM; grade 4) [2]. Several molecular markers, including *1p19q* codeletion and isocitrate dehydrogenase (*IDH*) mutation are instrumental in the classification, prognosis, and treatment of gliomas [3]. The 2021 World Health Organization (WHO) Classification of Tumors of the Central Nervous System subdivided adult-type diffuse glioma into three types based on histologic patterns and molecular markers: (1) astrocytoma, *IDH*-mutant; (2) oligodendroglioma, *IDH*-mutant, and *1p/19q*-codeleted; and (3) glioblastoma, *IDH*-wildtype [4]. The prognosis for patients with glioma remains poor, despite the availability of many treatment options, including surgical resection, chemotherapy, radiotherapy, and immunotherapy [5].

Small ubiquitin-related modifiers (SUMOs) are a large family of conserved proteins shared by all eukaryotic organisms [6]. SUMOylation is a posttranslational protein modification involved in several biological activities, including transcription and cell signaling [7]. A series of events mediated by the SUMO E1 activation enzyme, E2 conjugation enzyme, and several E3 ligases result in SUMOylation [8]. The essential elements of E1, responsible for the activation of protein SUMOylation, are SUMO-activating enzyme subunit 1 (SAE1) and ubiquitin-like modifier activating enzyme 2 (UBA2) [9]. Of note, several studies have shown that UBA2 expression is strongly correlated to the progression of pancreatic, lung, kidney, and colorectal cancers as well as being overexpressed in a variety of malignancies [7,10–14]. These findings imply that *UBA2* is a promising therapeutic target for the management of cancer. However, the role of *UBA2* in glioma is still unknown.

The aim of this research was therefore to clarify the expression level of UBA2 in glioma, as well as its clinicopathological correlations and prognostic significance. In addition, the correlation between UBA2 expression and drug sensitivity in cancer was also examined. To accomplish this, a bioinformatic analysis of various public databases was conducted. A series of *in vitro* cellular experiments further explored the function of *UBA2* in glioma. Individualized treatment of gliomas is still being investigated, and there is an urgent need for more research on different targets. The results of the present work show that *UBA2* is a promising prognostic biomarker and a potential therapeutic target in glioma. These findings may be important for the management of future glioma patients.

2. Materials and Methods

2.1 Data Collection, Preprocessing, and Expression Analysis

The UCSC Xena online tool (https://xenabrowser.net/datapages/) was used to compile data from the Cancer Genome Atlas (TCGA) and the Genotype-Tissue Expression (GTEx) RNAseq databases in transcripts per million (TPM) format, and together with prognostic data for glioma [15]. UBA2 protein levels were analyzed using the University of Alabama at Birmingham Cancer Data Analysis Portal (UALCAN, https://ualcan.path.uab.edu/), and the aforementioned results were verified using the Gene Expression Profiling Interactive Analysis (GEPIA, http://gepia.cancer-pku.cn/) database [16,17]. Finally, the diagnostic receiver operating characteristic (ROC) curve was used to determine the ability of UBA2 expression to distinguish between tumor and normal tissue. Youden's index was used to determine the cut-off value for UBA2 expression to classify tumor and non-tumor brain tissue.

2.2 Prognostic Value of UBA2 in Glioma and the Nomogram Prognostic Model

The median value of UBA2 mRNA expression in 698 glioma patients from the TCGA dataset was used as the cut-off value to classify patients into low and high expression groups. Kaplan-Meier (K-M) survival analysis was conducted using the R packages "survminer" and "survivor", and survival curves were plotted for both groups. The study endpoints were disease-specific survival (DSS), overall survival (OS), and progression-free interval (PFI). A cohort dataset was also retrieved from the Chinese Glioma Genome Atlas database (CGGA, http://www.cgga.org.cn/) in order to perform survival analysis [18]. Univariate analysis using Cox proportional risk regression modelling was first performed to study the link between UBA2 expression and OS. Other clinical and pathological prognostic factors were also evaluated. Subsequently, variables with p values < 0.1 were included in multivariate Cox regression analysis to determine independent correlates of OS. The results were visualized by drawing forest plots using the R package "ggplot2". To assist clinicians in predicting the OS of patients, we constructed a prediction model using the R package "rms" and drew a calibration curve. The nomogram allows visualization of the correlation between each predictor and survival outcome. Each predictor corresponds to a scale of scores, and the sum of the scores for all factors corresponds to the probability of OS at different times. We also developed and validated the DSS and PFI prediction models using the same approach.

2.3 Immune Cell Infiltration and the Tumor Microenvironment in Gliomas

Immune infiltration was first evaluated based on the single sample gene set enrichment analysis (ssGSEA) algorithm provided in the R package "Gene Set Variation Analysis (GSVA)" and using previously published markers for 24 immune cells types [19,20]. Subsequently, immune cell infiltration was determined using the xCELL, CIBERSORT, MCPcounter, and TIMER algorithms with the R package "IOBR" [20–26]. The stromal, immune, and estimate scores were then calculated using the R package "ESTIMATE" [19].

2.4 Prediction of Drug Sensitivity

The RNAs associated with Drug (RNAactDrug, http://bio-bigdata.hrbmu.edu.cn/RNAactDrug/) database was used to explore the relationship between UBA2 mRNA expression and drug sensitivity. This online tool contains the Cancer Cell Line Encyclopedia (CCLE), the Genomics of Drug Sensitivity in Cancer (GDSC, formerly known as CGP), and the CellMiner databases. The computational analysis of resistance (CARE) algorithm utilizes compound screening data to identify biomarkers of response to targeted therapies. This contains the Cancer Therapeutic Response Portal (CTRP), CCLE, and CGP databases, and results in a CARE score that reflects drug sensitivity [27].

2.5 Cell Culture

Three human glioma cell lines (A172, U251, and U87) and one human normal astrocyte cell line (HA1800) were investigated in this study. The glioma cell lines were obtained from the Institute of Modern Physics, Chinese Academy of Sciences (Lanzhou, China), while the HA1800 cell line was obtained from Mingzhoubio (Ningbo, China). Short Tandem Repeat (STR) analysis was performed to identify the cell lines. All the cell lines were mycoplasma-negative and were cultured at 37 °C with 5% CO_2 in Dulbecco's Modified Eagle Medium with 1% penicillin/streptomycin (Solarbio, Beijing, China) and 10% fetal bovine serum (FBS, ExCell Bio, Soochow, China).

2.6 RNA Interference

Lentiviruses containing short hairpin RNA targeting *UBA2* (shUBA2) and negative control (shNC) were obtained from Hanbio (Shanghai,

China). The shRNA sequences were: shUBA2-1, 5′-GCCTGATTGATCTGGATACTATTGAT-3′; shUBA2-2, 5′-GCCTAGGAAAGGACGTTGAATTTGAA-3′; and shNC, 5′-TTCTCCGAACGTGTCACGTAA-3′. U87 cells were transfected with shUBA2 or shNC lentiviruses in the presence of 1 µg/mL polybrene for 24 h. Stably transfected cells were selected 72 h later using 2 µg/mL puromycin.

2.7 Western Blotting

Total protein was extracted from cells using radioimmunoprecipitation assay lysis buffer containing a serine protease inhibitor (1% phenylmethylsulfonyl fluoride). Proteins were subsequently separated by electrophoresis on a 10% sodium dodecyl sulfate-polyacrylamide gel, and then transferred onto a polyvinylidene fluoride membrane (Millipore, Cork, Ireland). After blocking for 1 h in 5% non-fat milk in tris-buffered saline and Tween 20 (TBST, Solarbio, Beijing, China), the membrane was incubated overnight at 4 °C with primary antibody against β-actin (1:2000 20536-1-AP, Proteintech, Wuhan, China) or UBA2 (1:2000 ab185955, Abcam, Cambridge, UK). Following three TBST washes, the membranes were incubated for 1 h at room temperature with secondary antibodies, washed with TBST, and then developed with super enhanced chemiluminescence (ECL) detection reagent (Yeasen, Shanghai, China).

2.8 Quantitative Real-Time Polymerase Chain Reaction (qRT-PCR)

TRIzol reagent (Ambion, Carisbad, CA, USA) was used to extract total RNA from cells. This was then reverse transcribed to generate cDNA using the SweScript RT First Strand cDNA Synthesis Kit (Servicebio, Wuhan, China). Quantitative Real-Time Polymerase Chain Reaction (qRT-PCR) was conducted using Bio-rad CFX management and 2×SYBR Green qPCR Master Mix (Servicebio, Wuhan, China). The PCR primer sequences were: UBA2, forward 5′-GCTGGGTTGATAGTATTGGAAGG-3′ and reverse 5′-CTTTATGGACATTCAGCCGCAC-3′; β-actin, forward 5′-CACCCAGCACAATGAAGATCAAGAT-3′ and reverse 5′-CCAGTTTTTAAATCCTGAGTCAAGC-3′. The $2^{-\Delta\Delta Ct}$ method was employed to quantify mRNA levels, with β-actin serving as the internal control.

2.9 Cell Irradiation

Cells were irradiated using an X-RAY generator (X-RAD 225, North Branford, CT, USA). The dose rate was set to 2.0–3.0 Gy/min (225 KV/13.3 mA, 0.2 mm Al filter), and source-skin distance was 40 cm.

2.10 Colony Formation Assay

For the colony formation assay, a single cell suspension containing an appropriate number of cells was placed in 60-mm petri dishes. The medium was replaced every 4 days. After 2 weeks of incubation, the cells were fixed in ethanol and 0.1% concentration of crystal violet (Solarbio, Beijing, China) was used to stain the colonies.

2.11 Cell Counting Kit-8 (CCK-8) Assay

Cells were seeded at 4×10^3 cells/well into 96-well plates and 10 µL of Cell Counting Kit-8 (CCK-8) reagent (Yeasen, Shanghai, China) was added at 0, 24, 48, and 72 h to measure cell proliferation using the CCK-8 assay. After incubation for 2 h, absorbance was measured at a wavelength of 450 nm.

2.12 Cell Apoptosis and Cycle Assay

Cells were seeded into 6-well plates (2×10^5 cells per well) and grown for 48 h. Apoptosis was then measured using flow cytometry and an Annexin V-FITC/PI cell apoptosis analysis kit (Meilunbio, Dalian, China). For the cell cycle assay, cells were fixed in 70% ethanol at –20 °C overnight, stained with DNA staining solution (Liankebio, Hangzhou, China) at room temperature for 30 min, and evaluated by flow cytometry. Modfit LT software5.0.9 (Verity Software House, Bedford, MA, USA) was used to perform cell cycle analysis.

2.13 Cell Migration and Invasion Assay

The cell migration assay was performed using 24-well transwell chambers (Corning, Kennebunk, ME, USA). Briefly, 3×10^4 cells in serum-free medium were added to the upper chamber, and medium containing 15% FBS was added to the lower chamber. Upper chamber cells were removed after 24 h of culture with a damp cotton swab, fixed in methanol, and stained with 0.1% crystal violet (Solarbio, Beijing, China). For the cell invasion assay, the upper chamber was coated with 1:8 Matrigel (BD Biosciences, San Jose, CA, USA), and the remaining experimental procedure was similar to that of the cell migration assay. Finally, the invasive and migrated cells were photographed using a light microscope (Olympus, Tokyo, Japan).

2.14 Statistical Analysis

The student's *t* test or Mann–Whitney U rank-sum test was used to compare UBA2 expression between tumor and normal tissues, depending on the results of the normality test of the samples. These tests were also used to determine correlations between UBA2 expression and clinicopathological variables. The log-rank test was used to perform a K-M survival analysis. The Pearson or Spearman's test was used for correlation analysis. R software 4.2.1 (Ross Ihaka and Robert Gentleman, Auckland, New Zealand) and GraphPad Prism 9.4.0 (Dotmatics, Boston, MA, USA) were employed for all statistical calculations and data visualizations, with the specific R package described in the preceding sections. All *p*-values in this study were tested using a two-tailed test, with $p < 0.05$ denoting the statistical significance. All data was presented in the format of means ± standard deviation.

3. Results

3.1 UBA2 Overexpression in Glioma

Pan-cancer analysis of the TCGA-GTEx database revealed that UBA2 was overexpressed in multiple cancers relative to corresponding normal tissues, including glioma (Fig. 1A–C). In the GEPIA, UALCAN, and Clinical Proteomic Tumor Analysis Consortium (CPTAC, https://proteomics.cancer.gov/programs/cptac) databases, UBA2 expression was substantially higher in glioma compared to normal tissues (Fig. 1D–F). UBA2 protein and mRNA expression in glioma (A172, U251, and U87) and astrocyte (HA1800) cell lines were detected using Western blotting and quantitative real-time polymerase chain reaction (qRT-PCR) assays. Compared to the typical astrocyte cell line, glioma cell lines expressed significantly higher levels of UBA2 protein and mRNA (Fig. 1G,H). Furthermore, the diagnostic ROC curve showed that UBA2 expression could effectively differentiate between glioma and normal tissues (Area Under Curve = 0.867, Fig. 1I). The expression level of UBA2 was 5.81 at the maximum Youden's index, indicating this was the optimal cut-off value for distinguishing between glioma and normal tissues (**Supplementary Fig. 1**). These findings demonstrate that UBA2 is overexpressed in glioma cell lines and tissues.

3.2 The Relationship Between Glioma Clinicopathological Parameters and UBA2 Expression

The relationship between UBA2 expression and various clinicopathological parameters in glioma patients was analyzed using the TCGA database (**Supplementary Table 1**). UBA2 expression in glioma was associated with WHO grade, *IDH* gene status, histological type, and *1p19q* deletion, but not with patient sex, race, or age. UBA2 expression was higher in WHO grade 4 gliomas compared to WHO grade 2 and 3 gliomas (Fig. 2A). Additionally, UBA2 expression was higher in glioblastoma than in astrocytoma, oligoastrocytoma, and oligodendroglioma (Fig. 2C). Patients with *1p19q* non-codeletion and *IDH*-wildtype, both of which are indicators of poor prognosis, showed highly elevated expression of UBA2 (Fig. 2B,D). Together, these findings indicate that UBA2 expression is associated with the malignant progression of glioma.

3.3 High UBA2 Expression Predicts Poor Survival in Glioma Patients

K-M analysis to explore the association between UBA2 expression and survival in glioma patients from the TCGA database. Patients with high UBA2 expression showed significantly worse OS, PFI, and DSS than those with low UBA2 expression (Fig. 3A–C). Further subgroup analyses revealed that high UBA2 expression was associated with poorer OS in patients with WHO grade 2 glioma, oligodendroglioma, and *IDH* mutant glioma, as well as in both male and female patients, aged $\leq$60 years old, and White individuals (Fig. 3D–J). Similar results were obtained following analysis of data from the CGGA database (Fig. 4A,D,H–J). Notably, the association between UBA2 expression and OS in the CGGA database was also found in WHO grade 3 glioma, anaplastic astrocytoma, gliomas with *1p19q* non-codeletion, and glioma with methylated or unmethylated methylguanine methyltransferase (MGMT) promoter (Fig. 4B,C,E–G). These findings indicate that high UBA2 expression predictes poor survival in glioma patients.

3.4 UBA2 is a Prognostic Biomarker in Patients with Glioma

To further examine whether *UBA2* is a prognostic factor for glioma, data from the TCGA database was used to perform univariate and multivariate Cox regression analyses. *IDH* status, patient age, WHO grade, *1p19q* codeletion, sex, and UBA2 expression levels were all significantly associated with OS in univariate analysis (Fig. 5A). Multivariate analysis further revealed that patient age, *IDH* status, and WHO grade were independent prognostic factors (Fig. 5B). Next, a nomogram was constructed using WHO grade, *IDH* status, age, and UBA2 expression level to predict 1-year, 3-year, and 5-year OS in glioma patients (Fig. 5C). The calibration curve demonstrated consistency of the observed results with the predicted values (Fig. 5D). Using this method, nomograms for PFI and DSS and their respective calibration curves were also created (Fig. 5E–H). Taken together, these results indicate that *UBA2* is a promising prognostic biomarker for glioma.

3.5 Relationship Between UBA2 Expression and Tumor-Infiltrating Immune Cells in Glioma

In light of the prognostic significance of tumor-infiltrating immune cells in gliomas, we next evaluated whether UBA2 expression was related to immune cell infiltration. The ssGSEA computational tool was used to compare the distribution of 24 distinct immune cell subpopulations between the high and low UBA2 expression groups. As shown in Fig. 6A, activated dendritic cells (DC), induced DC, macrophages, neutrophils, T helper cells, gamma delta T cells, and T helper type 2 cells were markably increased in the high UBA2 expression group. In contrast, CD8 T cells, DC, mast cells, natural killer (NK) CD56 bright cells, NK CD56 dim cells, plasmacytoid DC, follicular helper T cells (Tfh), Th17 cells, and T-regulatory cells were markedly lower in the high UBA2 expression group (Fig. 6A). Validation was performed with four algorithms, all of which yielded the same results as above (Fig. 6B). The ImmuneScore, EstimateScore, and StromalScore values were all higher in the UBA2 high expression group compared to the low expression group, with all showing a positive linear correlation (Fig. 6C–H). These findings indicate that UBA2 expression is linked to immune cell infiltration in glioma.

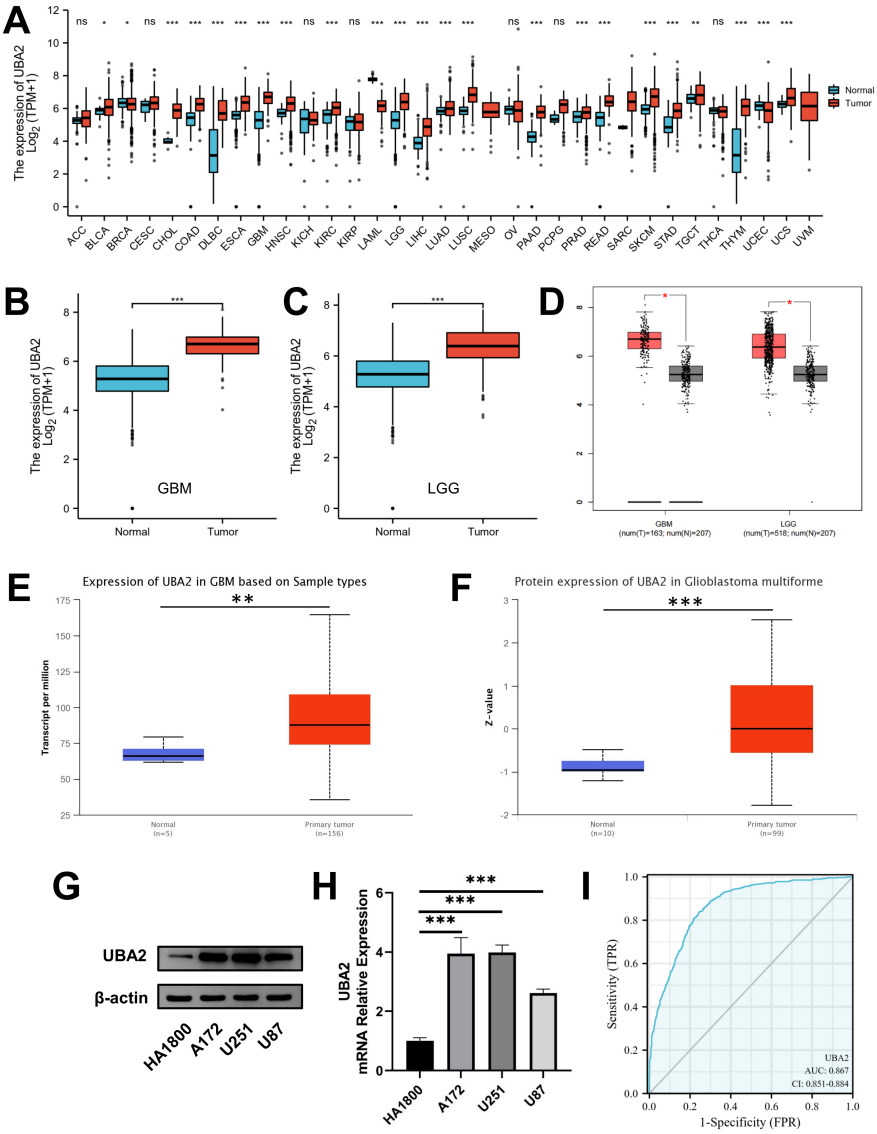

Fig. 1. Expression of UBA2 in glioma tissues and cell lines. UBA2 mRNA expression between tumor and normal samples in (A) pan-cancer, (B) GBM, and (C) LGG from TCGA and GTEx database. (D) UBA2 mRNA expression between tumor and normal samples in GBM and LGG from GEPIA database. (E) UBA2 mRNA expression in GBM between tumor and normal samples from UALCAN database. (F) UBA2 protein expression in glioblastoma between tumor and normal samples from CPTAC database. (G) Western blotting and (H) quantitative real-time PCR analysis of UBA2 in normal astrocyte and glioma cell lines (***$p < 0.001$, A172 vs HA1800, n = 3; ***$p < 0.001$, U251 vs HA1800, n = 3; ***$p < 0.001$, U87 vs HA1800, n = 3). (I) Diagnostic ROC curve of UBA2 by TCGA and GTEx database. (*$p < 0.05$, **$p < 0.01$, ***$p < 0.001$, ns presented no significance). UBA2, ubiquitin-like modifier activating enzyme 2; GBM, glioblastoma multiforme; TCGA, the Cancer Genome Atlas; GTEx, Genotype-Tissue Expression; GEPIA, Gene Expression Profiling Interactive Analysis; UALCAN, University of Alabama at Birmingham Cancer Data Analysis Portal; CPTAC, Clinical Proteomic Tumor Analysis Consortium; PCR, polymerase chain reaction; ROC, receiver operating characteristic; ACC, adrenocortical carcinoma; BLCA, bladder urothelial carcinoma; BRCA, breast invasive carcinoma; CESC, cervical squamous cell carcinoma and endocervical adeno carcinoma; CHOL, cholangio carcinoma; COAD, colon adenocarcinoma; DLBC, lymphoid neoplasm diffuse large B-cell lymphoma; ESCA, esophageal carcinoma; HNSC, head and neck squamous cell carcinoma; KICH, kidney chromophobe; KIRC, kidney renal clear cell carcinoma; KIRP, kidney renal papillary cell carcinoma; LAML, acute myeloid leukemia; LGG, low-grade glioma; LIHC, liver hepatocellular carcinoma; LUAD, lung adenocarcinoma; LUSC, lung squamous cell carcinoma; MESO, mesothelioma; OV, ovarian serous cystadenocarcinoma; PAAD, pancreatic adenocarcinoma; PCPG, pheochromocytoma and paraganglioma; PRAD, prostate adenocarcinoma; READ, rectum adenocarcinoma; SARC, sarcoma; SKCM, skin cutaneous melanoma; STAD, stomach adenocarcinoma; TGCT, testicular germ cell tumors; THCA, thyroid carcinoma; THYM, thymoma; UCEC, uterine corpus endometrial carcinoma; UCS, uterine carcinosarcoma; UVM, uveal melanoma; FPR, false positive rate; 95% CI, 95% confidence interval.

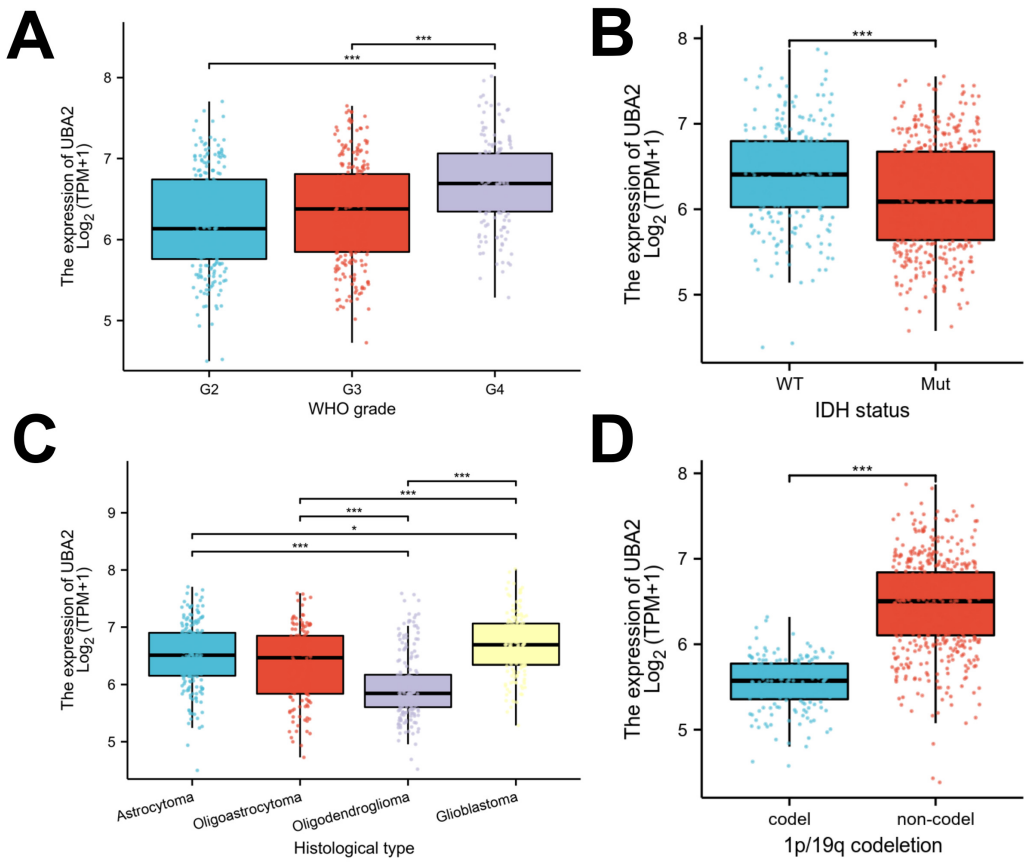

Fig. 2. Associations between UBA2 expression and clinicopathological parameters. Violin plots indicating UBA2 expression in different (A) WHO grade, (B) *IDH* status, (C) histological type, and (D) *1p/19q* co-deletion status from the TCGA database. (*$p < 0.05$, ***$p < 0.001$). WHO, World Health Organization; IDH, isocitrate dehydrogenase; TPM, transcripts per million; WT, wildtype.

3.6 Relationship Between UBA2 Expression and Drug Sensitivity

The relationship between UBA2 expression and drug sensitivity was analyzed using the RNAactDrug database. The calculated values showed a relationship between UBA2 expression and the IC50 of drugs. Sensitivities to Nilotinib, Erlotinib, Panobinostat, Sorafenib, Topotecan, and Irinotecan were all positively associated with UBA2 expression (Fig. 7A). A total of 6, 124, and 35 compounds from the CCLE, CTRP, and CGP databases, respectively, were screened by CARE (Fig. 7B). Twenty of these compounds contained in at least two of the databases were selected for visualization and to label their targets, including drugs such as Nilotinib, Sorafenib, Axitinib, Vorinostat, Linifanib, Navitoclax, Cabozantinib, Imatinib, Quizartinib, Abraxane, Topotecan, and Panobinostat. These drugs are already on the market or have been used in clinical trials (Fig. 7C). The findings show that UBA2 expression is associated with the drug sensitivity of cancers.

3.7 UBA2 Knockdown Inhibits U87 Cell Progression

To further examine the involvement of *UBA2* in glioma development, lentiviruses carrying short hairpin RNA were used for stable knockdown of *UBA2* in U87 cells (shUBA2-U87) and for the negative control (shNC-U87). Both the protein and mRNA levels of UBA2 were markedly lower in shUBA2-U87 cells, as determined by Western blotting and qRT-PCR (Fig. 8A,B). U87 cells with the shUBA2-1 sequence were selected for subsequent experiments. The CCK-8 assay showed that knockdown of *UBA2* significantly slowed the proliferation of U87 cells (Fig. 8C). shUBA2-U87 cells also showed fewer colonies in the colony formation assay (Fig. 8D). The cell apoptosis assay revealed a significantly higher number of apoptotic shUBA2-U87 cells compared to shNC-U87 cells, suggesting that silencing of *UBA2* plays a role in cell apoptosis (Fig. 8E). *UBA2* knockdown in U87 cells significantly increased G0/G1 phase cells observed in the cell cycle assay, while reducing the S phase cells (Fig. 8F). Furthermore, shUBA2-U87 cells showed greatly reduced migration and invasion capacities (Fig. 8G). Taken together, these findings demonstrate that *UBA2* knockdown suppresses the progression of glioma cells.

3.8 UBA2 Knockdown Sensitizes U87 Cells to Irradiation

The CGGA database was used to determine whether UBA2 expression was associated with the outcome of

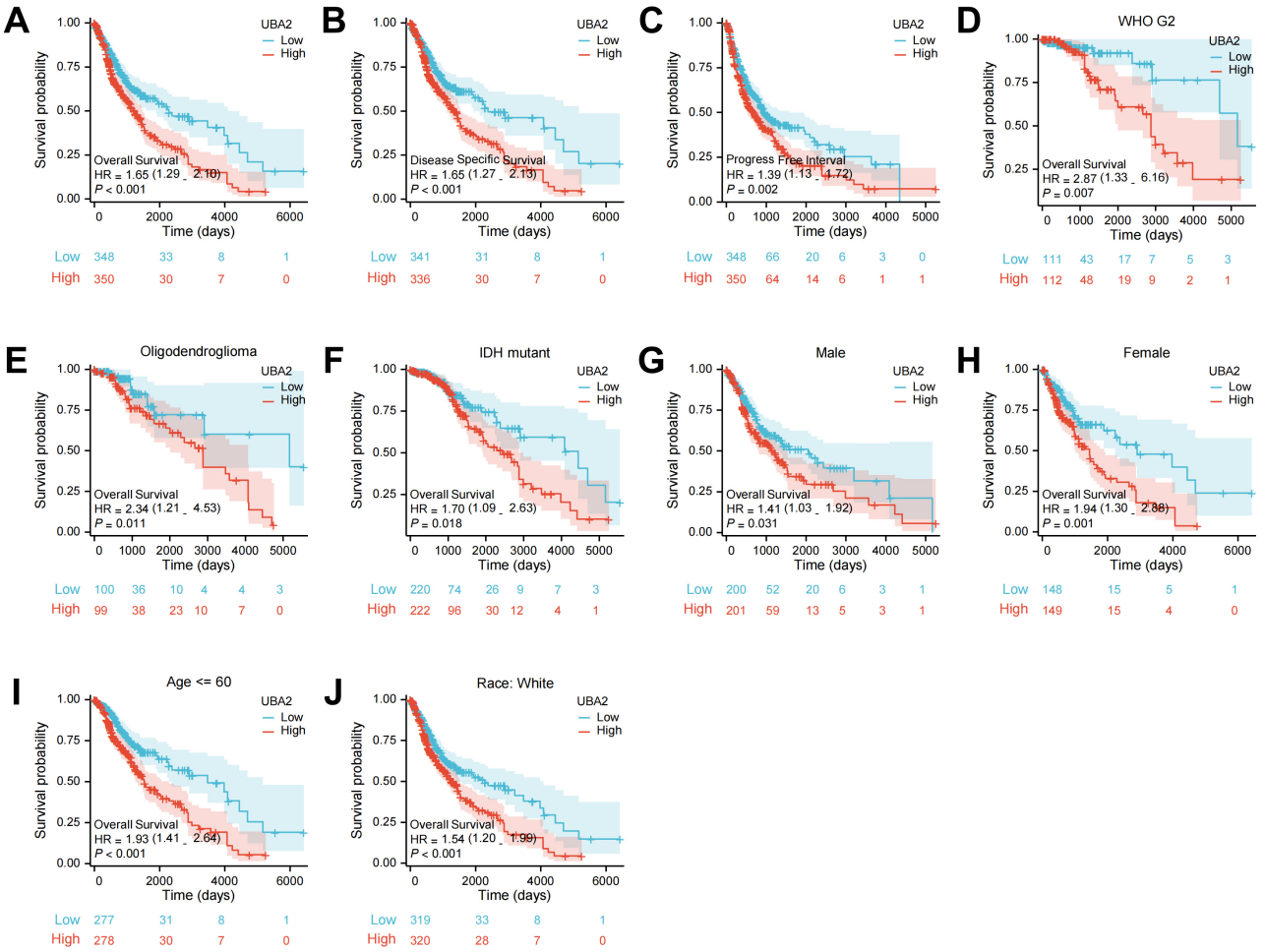

Fig. 3. The survival curves of UBA2 high- and low-expression groups in glioma patients from TCGA database. The survival curves of (A) OS, (B) PFS, and (C) DSS. The survival curves of OS in (D) WHO grade 2, (E) oligodendroglioma, (F) *IDH*-mutation, both (G) male and (H) female, (I) age $\leq$60, and (J) white subgroups. OS, overall survival; PFS, progression-free survival; DSS, disease-specific survival.

glioma patients after radiotherapy. Individuals with high UBA2 expression levels had a markedly poorer prognosis compared to those with low expression (Fig. 9A). We also investigated whether *UBA2* knockdown would sensitize glioma cells to irradiation. The colony formation assay and CCK-8 assay revealed that *UBA2* knockdown together with irradiation suppressed cell colony formation and proliferation (Fig. 9B,C). Moreover, the cell apoptosis assay revealed a higher apoptotic rate in irradiated shUBA2-U87 cells than in irradiated shNC-U87 cells (Fig. 9D). In summary, these findings imply that *UBA2* knockdown can sensitize glioma cells to irradiation.

4. Discussion

Gliomas are a large group of heterogeneous neurological tumors. The typing of gliomas is becoming clearer thanks to advances in molecular genetic testing and several clinical trials. Traditional and new treatment protocols are becoming more precise and standardized. These usually involve comprehensive assessment of the patient's clinical presentation, general condition, prognostic factors, and side effects after surgery and chemoradiotherapy. The results of molecular pathology and genetic examinations can provide important prognostic information, as well as guiding the choice of radiotherapy and chemotherapy. Mutations in *IDH1* and *IDH2* are associated with favorable prognosis, and patients with these mutations respond better to alkylating agents and radiotherapy [28]. The combined deletion of chromosome *1p19q* is also thought to be a favorable prognostic indicator and a predictor of greater sensitivity to radiotherapy and alkylating agents [29]. Methylation of the MGMT promoter in glioblastoma also indicates favorable prognosis and a positive therapeutic effect of temozolomide [30]. Several other molecular markers such as *H3K27*, *H3G34*, a-thalassemiamentalretardation syndrome X (*ATRX*), telomerase reverse tranase (*TERT*), and *miR181d* have also been shown to have both diagnostic and prognostic value.

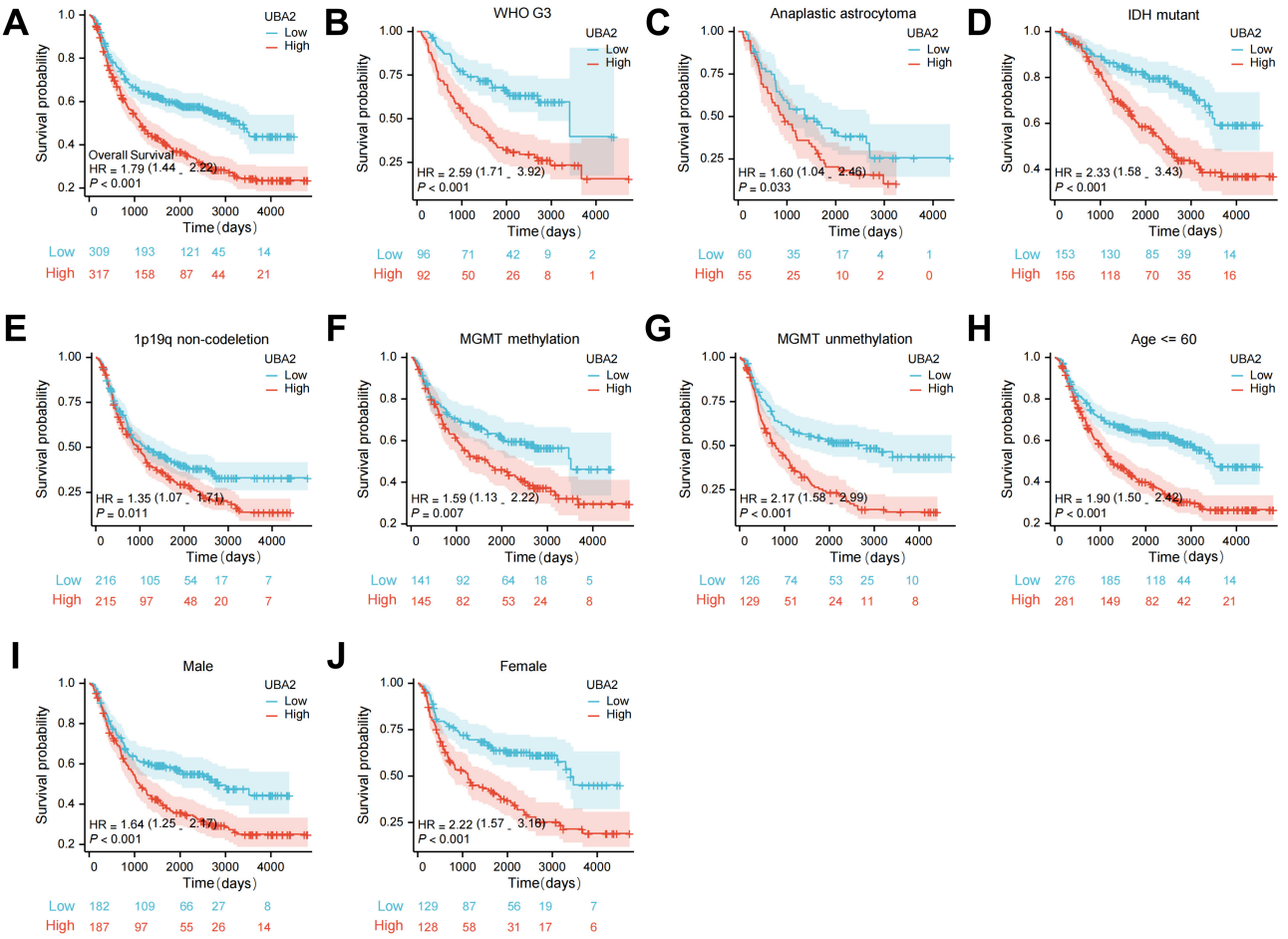

Fig. 4. The survival curves of UBA2 high- and low-expression groups in glioma patients from CGGA database. (A) The survival curves of OS. The survival curves of OS in (B) WHO grade 3, (C) anaplastic astrocytoma, (D) *IDH*-mutation, (E) *1p/19q* non-codeletion, both (F) MGMT methylation and (G) unmethylation, (H) age $\leq$60, and both (I) male and (J) female subgroups. MGMT, methylguanine methyltransferase.

4.1 Role of UBA2 in Malignant Tumors

Several previous studies have reported on the role of *UBA2* in tumor development. Zhang *et al.* [14] found that inhibition of UBA2 in clear cell renal cell carcinoma suppressed cell growth, induced apoptosis, and reduced the level of crucial enzymes associated with the *p53* mutant, *c-Myc*, and SUMO modification systems. He *et al.* [12] reported that *UBA2* knockdown in colorectal cancer cells reduced cell proliferation and concurrently increased cell apoptosis through regulation of the P53/murine double minute2 (MDM2)/P21 and phosphatase and tensin homolog deleted on chromosome ten (PTEN)/phosphoinositide 3-kinase (PI3K)/protein kinase B (AKT) signaling pathways. Li *et al.* [31] reported that knockdown of UBA2 inhibited the invasion and migration of gastric cancer cells by regulating the Wnt/β-catenin signaling pathway. In the present study, the majority of malignant tumors expressed high levels of UBA2. Our bioinformatic analysis and *in vitro* experiments showed that glioma tissue and cell lines expressed high levels of UBA2. Similar to the previous studies, we found that knockdown of *UBA2* reduced the ability of glioma cells to proliferate, migrate, and invade, while also enhancing apoptosis and G0/G1 cell cycle arrest. UBA2 expression correlated strongly with *IDH* status, histological type, WHO grade, and *1p19q* codeletion status. Patients with high UBA2 expression had worse prognosis than those with low expression. UBA2 expression could effectively differentiate tumors from normal tissue, and predict OS, PFI, and DSS in glioma patients. These results indicate that *UBA2* may be a potentially useful diagnostic and prognostic biomarker for glioma. Additionally, we found that UBA2 expression is linked to drug sensitivity in cancers, suggesting that it may be a useful target for drug therapy in tumors, including glioma.

4.2 Immunotherapy of Gliomas and the Potential Role of UBA2

Immune cell infiltration and immune regulation play a significant role in influencing the prognosis of glioma [32]. Increased expression levels of inhibitory checkpoint pro-

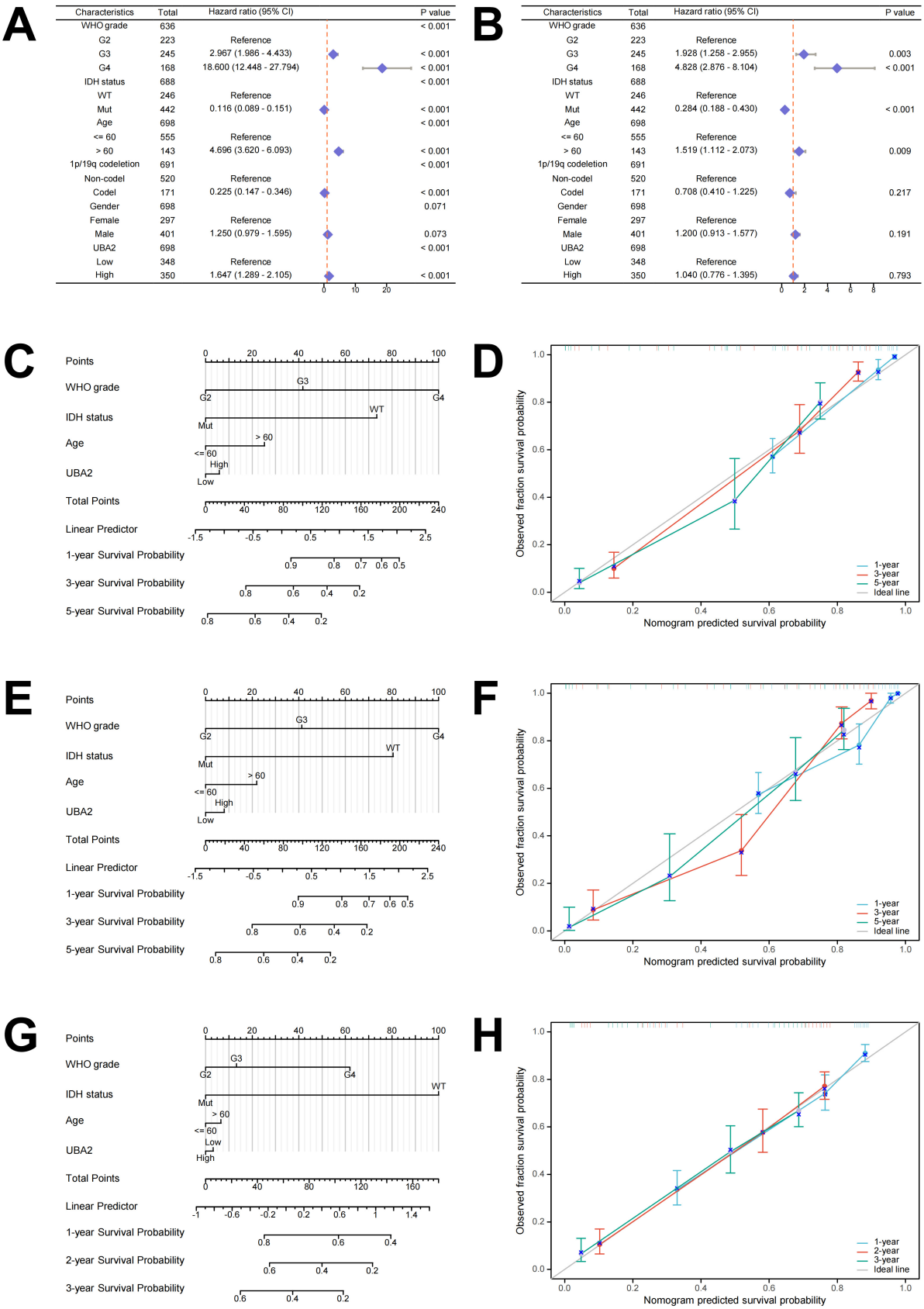

Fig. 5. The prognostic value of UBA2 in glioma. (A) Univariate and (B) multivariate Cox hazard regression analyses in glioma. (C) Nomogram and (D) calibration curves of 1-, 3-, and 5-year OS probabilities. (E) Nomogram and (F) calibration curves of 1-, 3-, and 5-year PFI probabilities. (G) Nomogram and (H) calibration curves of 1-, 2-, and 3-year DSS probabilities. PFI, progression-free interval.

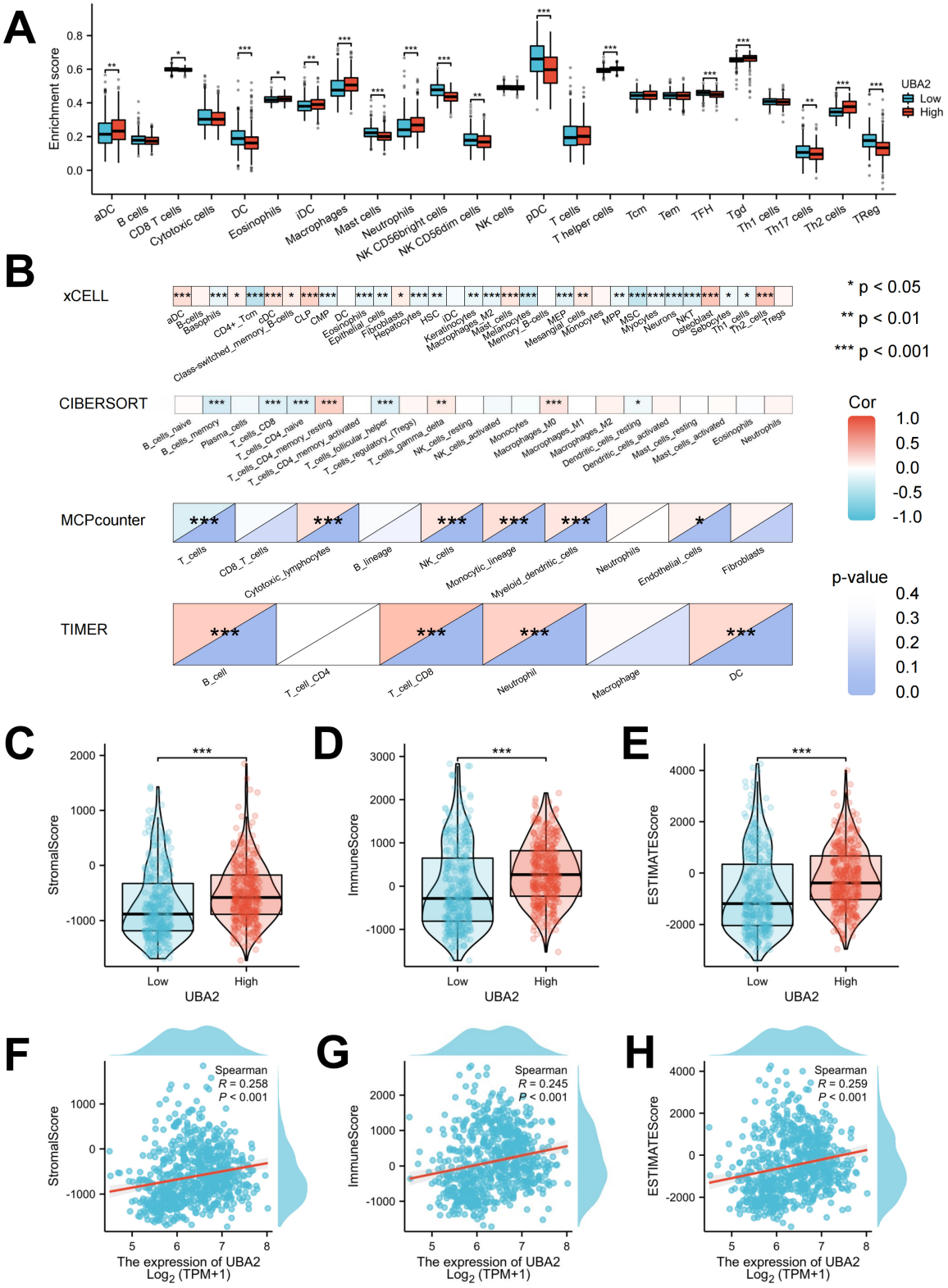

Fig. 6. Evaluation of the proportions of immune cell infiltration. (A) Immune cell distribution between tumor and normal tissues by ssGSEA. (B) Correlation patterns of infiltrating immune cells by 4 different algorithms. Correlation of UBA2 expression with (C,F) stromal, (D,G) immune, and (E,H) ESTIMATE scores. (*$p < 0.05$, **$p < 0.01$, ***$p < 0.001$). ssGSEA, single sample gene set enrichment analysis; DC, dendritic cells; NK, natural killer; TFH, follicular helper T; CLP, common lymphoid progenitor; CMP, common myeloid progenitor; HSC, hematopoietic stem cells; MPP, multipotent progenitor; MSC, mesenchymal stem cells; NKT, natural killer T; MCP, mast cell progenitor.

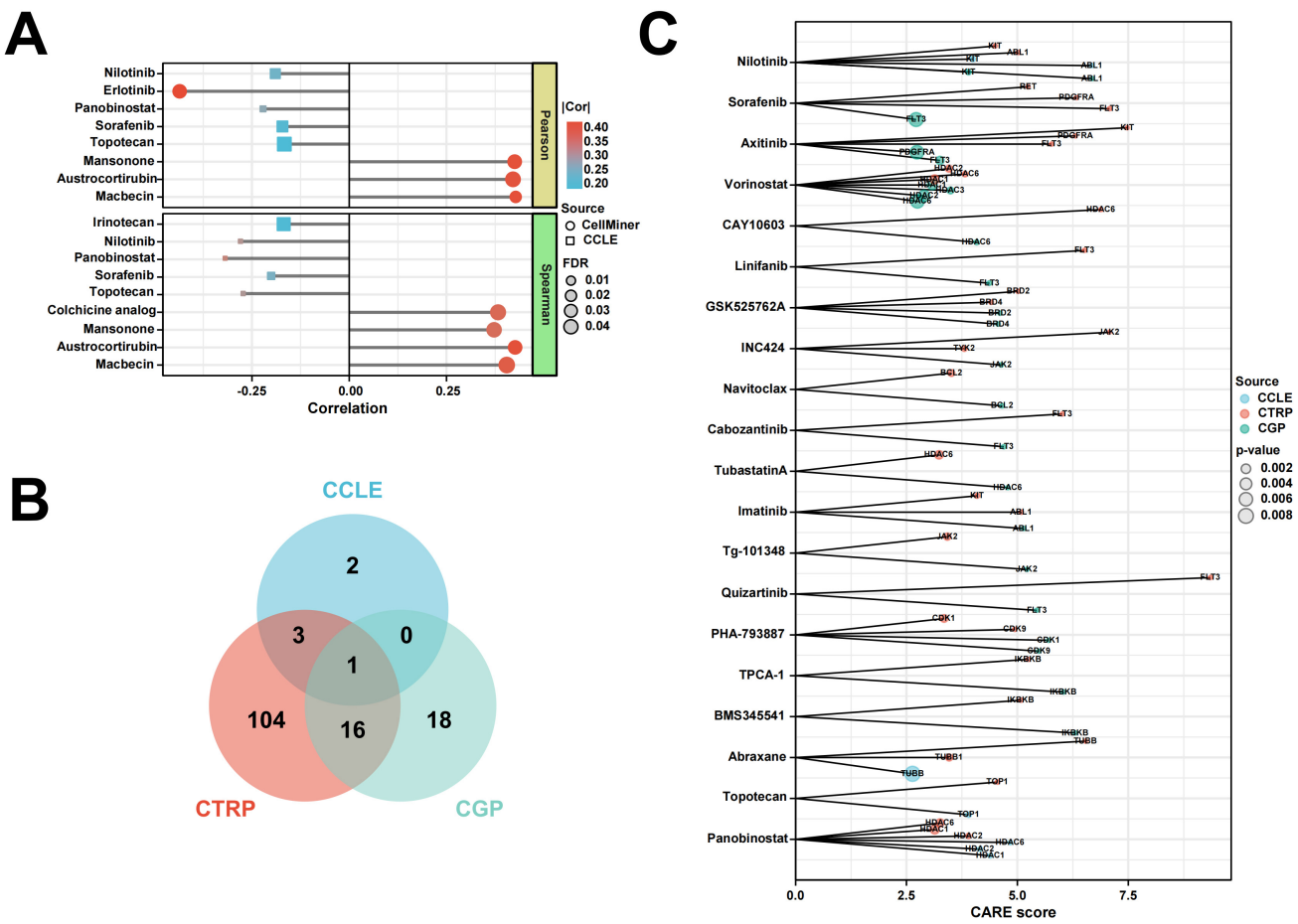

Fig. 7. Relationship between UBA2 expression and drug sensitivity. (A) Lollipop chart shows the correlation between UBA2 expression and drug sensitivity of tumor cells by RNAactDrug. (B) Venn diagram indicates the shared drug of three source using CARE. (C) Visualization of drugs overlapping in (B) and labeling of their targets. CCLE, Cancer Cell Line Encyclopedia; CTRP, Cancer Therapeutic Response Portal; CARE, Computational Analysis of Resistance.

teins, programmed cell death protein 1 (PD-1) (and its ligand PD-L1), and cytotoxic T lymphocyte-associated protein 4 (CTLA-4) have been correlated with immune evasion, elevated tumor grade, and poor prognosis in glioma patients [33]. However, immunotherapy for glioma remains challenging. Nivolumab and pembrolizumab have proven effective in other solid tumors and are now commonly used immune checkpoint inhibitors. However, both have failed to improve OS in several clinical trials of glioma [34–36]. Immunotherapy for glioma is still being explored, with the main focus currently being on immune checkpoint inhibitors. Recruitment has been completed for a clinical trial of ipilimumab with temozolomide versus temozolomide alone after surgery and chemoradiotherapy in GBM (Ipi-Glio/NCT02311920) [37]. In addition to PD-1/PD-L1 and CTLA-4, clinical trials that target other immune checkpoints such as T-cell immunoglobulin and mucin domain 3 (*TIM3*) and lymphocyte-activation gene 3 (*LAG3*) are currently ongoing (NCT02658981 and NCT02817633). These will not be discussed further here as several comprehensive reviews have recently summarized the topic of immunotherapy for glioma, we will not go into detail [38–40]. The current study found that UBA2 expression was significantly correlated with immune cell infiltration and the tumor microenvironment. This suggests that UBA2 is a key player in immune regulation and may also reflect the status of the immune microenvironment in gliomas. Furthermore, it suggests that *UBA2* may be a biomarker of the response to immune checkpoint inhibitors in gliomas, as well as affecting their efficacy.

4.3 UBA2 and Radiosensitization in Gliomas

Although radiotherapy is one of the standard treatment modalities for glioma, its efficacy is limited by radioresistance [41]. New approaches are therefore needed to improve the efficacy of radiotherapy for glioma. Several studies have shown that SUMOylation or SUMO targets are associated with the development of radioresistance in several tumor types. SUMO-interacting motif mimetic peptides coupled to gold nanoparticles have been observed to inhibit polySUMO-2/3-dependent protein-protein interactions [10]. The mechanism by which the SUMO path-

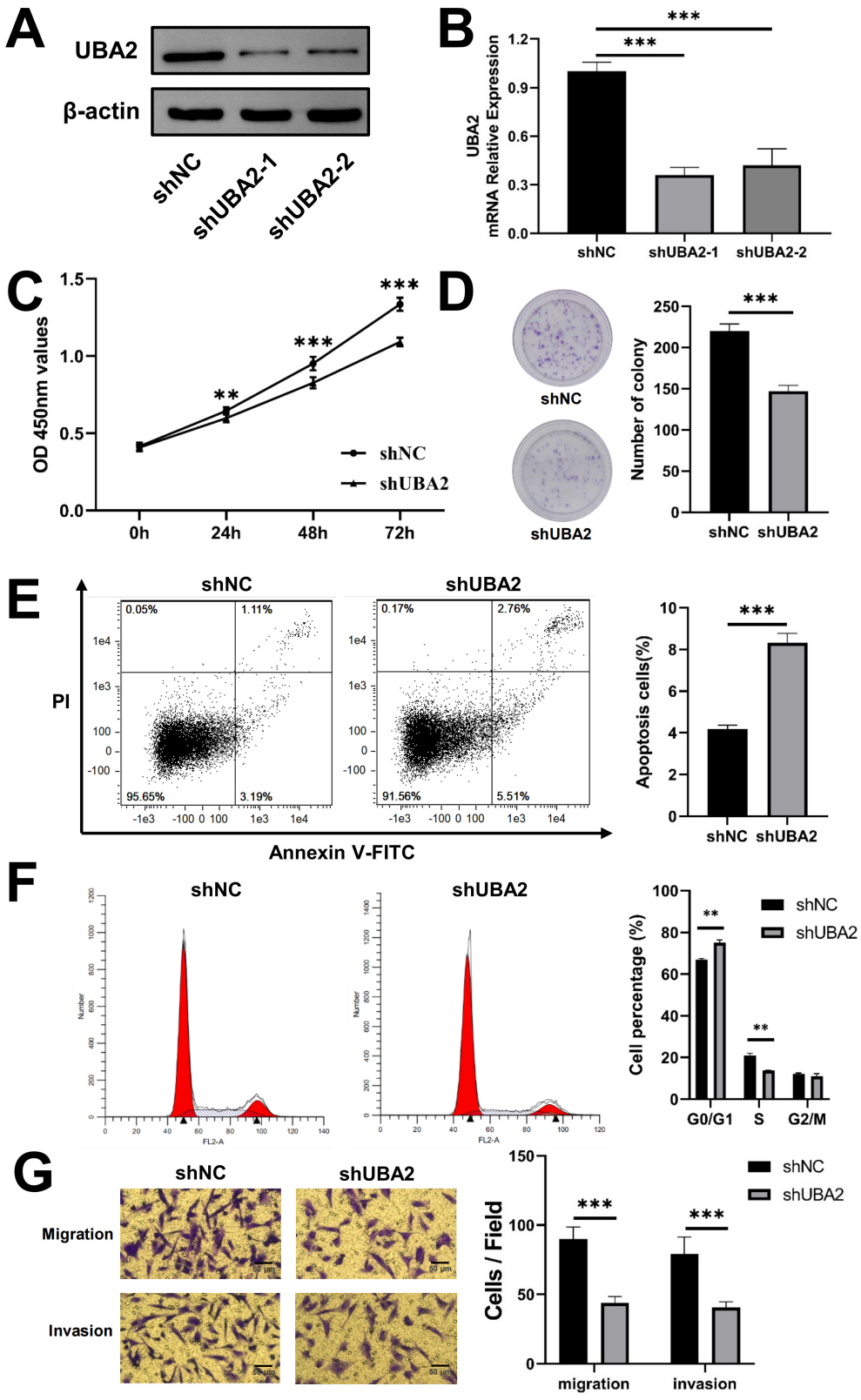

Fig. 8. Knockdown of *UBA2* inhibited U87 cells progression. (A) Western blotting, (B) quantitative real-time PCR (***$p < 0.001$, shUBA2-1 vs shNC, n = 3; ***$p < 0.001$, shUBA2-2 vs shNC, n = 3), (C) CCK-8 (**$p < 0.01$, shUBA2 vs shNC, 24 h, n = 6; ***$p < 0.001$, shUBA2 vs shNC, 48 h, n = 6; ***$p < 0.001$, shUBA2 vs shNC, 72 h, n = 6), (D) colony formation (***$p < 0.001$, shUBA2 vs shNC, n = 3), (E) cell apoptosis (***$p < 0.001$, shUBA2 vs shNC, n = 3), (F) cell cycle (**$p < 0.01$, shUBA2 vs shNC, G0/G1 stage, n = 3; **$p < 0.01$, shUBA2 vs shNC, S stage, n = 3), and (G) cell migration and invasion assays (400×) (***$p < 0.001$, shUBA2 vs shNC, migration, n = 3; ***$p < 0.001$, shUBA2 vs shNC, invasion, n = 3) in shNC and shUBA2. CCK-8, Cell Counting Kit-8.

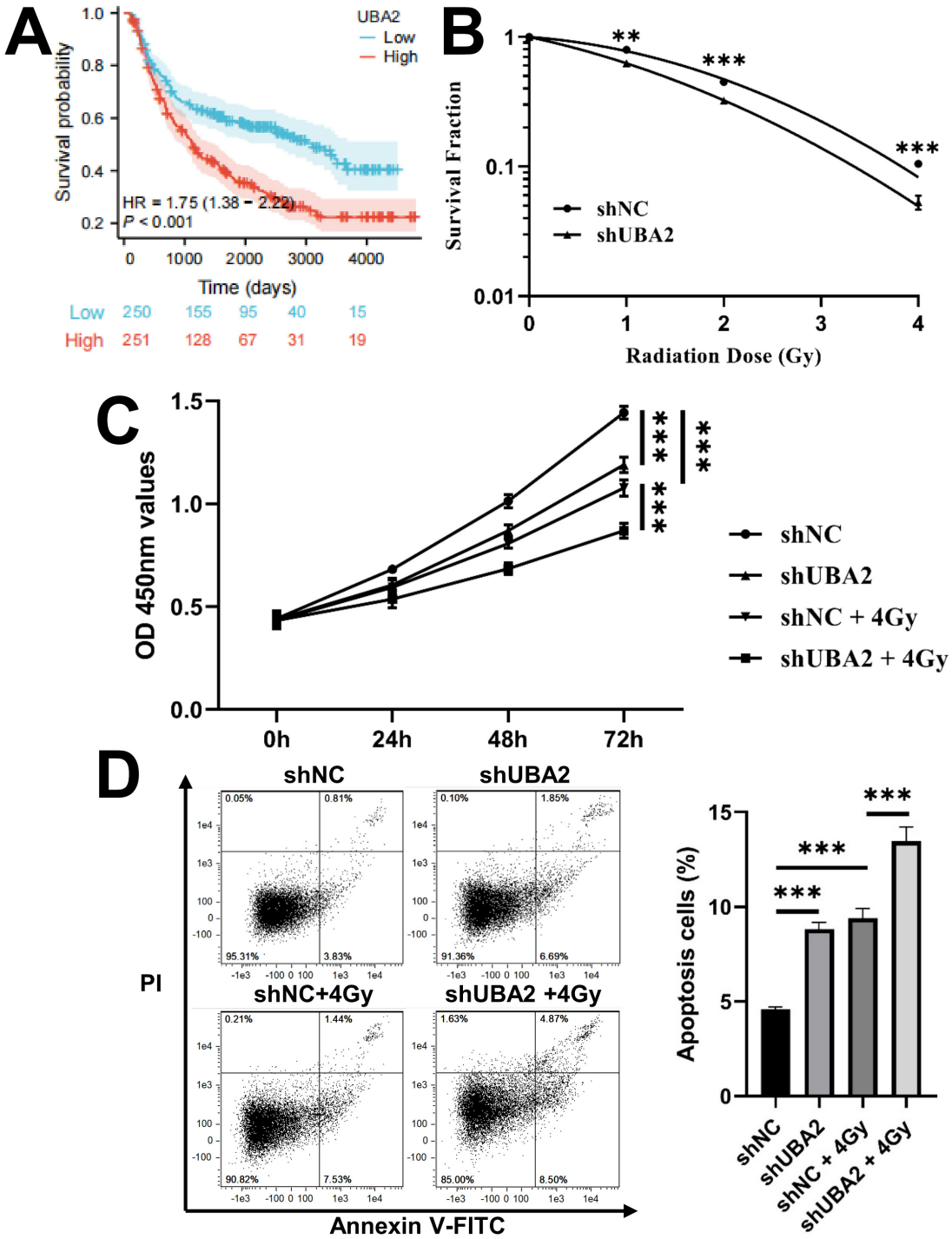

Fig. 9. Knockdown of *UBA2* sensitized U87 cells to irradiation. (A) The survival curves of OS in glioma patients treated with radiotherapy from CGGA database. (B) Survival fraction of shNC and shUBA2 at different irradiation doses (**$p < 0.01$, shUBA2 vs shNC, 1 Gy, n = 3; ***$p < 0.001$, shUBA2 vs shNC, 2 Gy, n = 3; ***$p < 0.001$, shUBA2 vs shNC, 4 Gy, n = 3). (C) CCK-8 (***$p < 0.001$, shUBA2 vs shNC, 72 h, n = 6; ***$p < 0.001$, shUBA2+4 Gy vs shNC+4 Gy, 72 h, n = 6; ***$p < 0.001$, shNC+4 Gy vs shNC, 72 h, n = 6) and (D) cell apoptosis assays in shNC and shUBA2 or in combination with 4 Gy irradiation (***$p < 0.001$, shUBA2 vs shNC, n = 3; ***$p < 0.001$, shNC+4 Gy vs shNC, n = 3; ***$p < 0.001$, shUBA2+4 Gy vs shNC, n = 3), respectively (***$p < 0.001$). HR, hazard ratio; OD, optical density; PI, propidium iodide; FITC, fluorescein isothiocyanate.

way sensitizes cancer cells to irradiation could therefore be via control of the DNA damage response. SUMO-specific proteases modulate the radiosensitivity of cancer cells through their involvement in various cellular processes [42–45]. Additionally, the combination of SUMOylation inhibitors such as 2-D08 and ML-792 with radiotherapy

may improve the outcome of cancer patients [46]. SAE1 or UBA2 is a subunit of the E1-activating enzyme involved in the SUMOylation of numerous proteins. The results of the present study are similar to a previous investigation which found that knockdown of *SAE1* enhanced the radiosensitivity of colorectal cancer cells [47]. We found that knockdown of *UBA2* sensitized glioma cells to irradiation, indicating that it may be a target for the radiosensitization of gliomas.

4.4 Strengths and Limitations

To our knowledge, this is the first study to correlate the expression of UBA2 in glioma with clinicopathological factors, immune cell infiltration, drug sensitivity, and radiosensitivity. UBA2 is overexpressed in gliomas, and is also closely associated with *IDH* status, histological type, WHO grade, and *1p19q* codeletion status. The prognosis of glioma patients with high UBA2 expression is worse than that of patients with low expression. These findings suggest that UBA2 expression is associated with the progression of gliomas and patient outcomes. It is well-known that the occurrence and advancement of glioma are related to immune cell infiltration, which has been shown to influence tumor progression and prognosis [48]. Our results showed that UBA2 expression was positively correlated with several immune cell types, including macrophages, neutrophils, activated DC, induced DC, and T helper cells, but negatively correlated with CD8 T cells, DC, mast cells, NK CD56 bright cells, and NK CD56 dim cells. These findings suggest that *UBA2* might participate in regulating immune cell infiltration in glioma. The major tumor-infiltrating cells are macrophages and neutrophils, and the infiltration and polarization of these cells are the main causes of chemotherapy and radiation resistance in gliomas [49]. Glioma-associated macrophages (GAMs) act critically in enhancing tumor progression and can alter drug resistance, promoting resistance to radiotherapy and establishing an immunosuppressive environment [50,51]. The current study showed that UBA2 expression was related to drug sensitivity in cancers, including glioma. The efficacy of radiotherapy in glioma appears to be constrained by cellular resistance to irradiation [41], with the present study finding that *UBA2* knockdown sensitized glioma cells to irradiation. In summary, it seems reasonable to speculate that *UBA2* might be involved in drug and irradiation resistance by regulating immune cell infiltration in gliomas.

Several potential biases and shortcomings of this study must be addressed prior to clinical translation. Firstly, public databases such as TCGA and CGGA, contain only limited clinical information. In particular, they lack data on surgical margins/extent of resection, which is a key determinant of prognosis. Moreover, the TCGA database contains only GBM and LGG cohorts. Despite these being the predominant pathological types, they are not completely representative of glioma. In order to validate our findings, future studies should include a larger size of clinical samples and more detailed clinical information. Secondly, the involvement of *UBA2* in glioma was not fully elucidated, and further investigations into the molecular mechanisms involved are warranted.

5. Conclusions

This study found that *UBA2* has diagnostic and prognostic value in glioma. *UBA2* may also be associated with tumor progression, immune cell infiltration, drug sensitivity, and radiosensitivity in glioma. It could therefore be a potential target for therapy, as well as a biomarker for the diagnosis, prognosis, immune response, drug sensitivity, and radiosensitivity of gliomas. This study provides new insights into the role of UBA2 in the growth and regulation of gliomas. The findings should contribute to the individualized treatment of glioma and may also help to guide clinical practice.

Availability of Data and Materials

The datasets generated during and/or analyzed during the current study are available from the corresponding author on reasonable request.

Author Contributions

YO and TD contributed to the conceptualization, methodology, software, validation, formal analysis, investigation, resources, data curation, writing—original draft preparation, writing—review and editing, and visualization; RL, DW, JC, MD, YW, and ZY contributed to the data curation, HL, QZ, and XW contributed to the conceptualization, supervision and project administration. All authors contributed to editorial changes in the manuscript. All authors read and approved the final manuscript. All authors have participated sufficiently in the work and agreed to be accountable for all aspects of the work.

Ethics Approval and Consent to Participate

Not applicable.

Acknowledgment

We appreciate all the authors who contributed to this study.

Funding

The study was supported by the National Key Research and Development Program of China (No. 2022YFC2401500), Science and Technology Plan Project of Chengguan District of Lanzhou (No. 2020-2-2-5), Talent Innovation and Venture Project of Lanzhou City (No. 2017-RC-23; 2021-RC-125; 2020-RC-113), China Foundation for International Medical Exchange (No. Z-2017-24-2108), Gansu Province Project of Science and Technologies (Grant No. 20JR10RA680), and the Lanzhou heavy Ion Accelerator High-end user Project (HIR20GY007).

Conflict of Interest

The authors declare no conflict of interest.

Supplementary Material

Supplementary material associated with this article can be found, in the online version, at https://doi.org/10.31083/j.fbl2904144.

References

[1] Ostrom QT, Patil N, Cioffi G, Waite K, Kruchko C, Barnholtz-Sloan JS. CBTRUS Statistical Report: Primary Brain and Other Central Nervous System Tumors Diagnosed in the United States in 2013–2017. Neuro-oncology. 2020; 22: iv1–iv96.

[2] Louis DN, Perry A, Reifenberger G, von Deimling A, Figarella-Branger D, Cavenee WK, *et al*. The 2016 World Health Organization Classification of Tumors of the Central Nervous System: a summary. Acta Neuropathologica. 2016; 131: 803–820.

[3] Reifenberger G, Wirsching HG, Knobbe-Thomsen CB, Weller M. Advances in the molecular genetics of gliomas - implications for classification and therapy. Nature Reviews. Clinical Oncology. 2017; 14: 434–452.

[4] Louis DN, Perry A, Wesseling P, Brat DJ, Cree IA, Figarella-Branger D, *et al*. The 2021 WHO Classification of Tumors of the Central Nervous System: a summary. Neuro-oncology. 2021; 23: 1231–1251.

[5] Xu S, Tang L, Li X, Fan F, Liu Z. Immunotherapy for glioma: Current management and future application. Cancer Letters. 2020; 476: 1–12.

[6] Eifler K, Vertegaal ACO. Mapping the SUMOylated landscape. The FEBS Journal. 2015; 282: 3669–3680.

[7] Du X, Shi J. UBA2 promotes the progression of renal cell carcinoma by suppressing the p53 signaling. Irish Journal of Medical Science. 2022; 191: 1555–1560.

[8] Chen Y. A new immuno-oncology target - SUMOylation. Trends in Cancer. 2023; 9: 606–608.

[9] Wilson VG. Introduction to Sumoylation. Advances in Experimental Medicine and Biology. 2017; 963: 1–12.

[10] Schneeweis C, Hassan Z, Schick M, Keller U, Schneider G. The SUMO pathway in pancreatic cancer: insights and inhibition. British Journal of Cancer. 2021; 124: 531–538.

[11] Jiang B, Fan X, Zhang D, Liu H, Fan C. Identifying UBA2 as a proliferation and cell cycle regulator in lung cancer A549 cells. Journal of Cellular Biochemistry. 2019; 120: 12752–12761.

[12] He P, Sun X, Cheng HJ, Zou YB, Wang Q, Zhou CL, *et al*. UBA2 promotes proliferation of colorectal cancer. Molecular Medicine Reports. 2018; 18: 5552–5562.

[13] Cheng H, Sun X, Li J, He P, Liu W, Meng X. Knockdown of Uba2 inhibits colorectal cancer cell invasion and migration through downregulation of the Wnt/β-catenin signaling pathway. Journal of Cellular Biochemistry. 2018; 119: 6914–6925.

[14] Zhang G, Zou J, Shi J, Qian B, Qiu K, Liu Q, *et al*. Knockdown of ubiquitin-like modifier-activating enzyme 2 promotes apoptosis of clear cell renal cell carcinoma cells. Cell Death & Disease. 2021; 12: 1067.

[15] Vivian J, Rao AA, Nothaft FA, Ketchum C, Armstrong J, Novak A, *et al*. Toil enables reproducible, open source, big biomedical data analyses. Nature Biotechnology. 2017; 35: 314–316.

[16] Chandrashekar DS, Bashel B, Balasubramanya SAH, Creighton CJ, Ponce-Rodriguez I, Chakravarthi BVSK, *et al*. UALCAN: A Portal for Facilitating Tumor Subgroup Gene Expression and Survival Analyses. Neoplasia (New York, N.Y.). 2017; 19: 649–658.

[17] Chandrashekar DS, Karthikeyan SK, Korla PK, Patel H, Shovon AR, Athar M, *et al*. UALCAN: An update to the integrated cancer data analysis platform. Neoplasia (New York, N.Y.). 2022; 25: 18–27.

[18] Zhao Z, Zhang KN, Wang Q, Li G, Zeng F, Zhang Y, *et al*. Chinese Glioma Genome Atlas (CGGA): A Comprehensive Resource with Functional Genomic Data from Chinese Glioma Patients. Genomics, Proteomics & Bioinformatics. 2021; 19: 1–12.

[19] Yoshihara K, Shahmoradgoli M, Martínez E, Vegesna R, Kim H, Torres-Garcia W, *et al*. Inferring tumour purity and stromal and immune cell admixture from expression data. Nature Communications. 2013; 4: 2612.

[20] Bindea G, Mlecnik B, Tosolini M, Kirilovsky A, Waldner M, Obenauf AC, *et al*. Spatiotemporal dynamics of intratumoral immune cells reveal the immune landscape in human cancer. Immunity. 2013; 39: 782–795.

[21] Zeng D, Ye Z, Shen R, Yu G, Wu J, Xiong Y, *et al*. IOBR: Multi-Omics Immuno-Oncology Biological Research to Decode Tumor Microenvironment and Signatures. Frontiers in Immunology. 2021; 12: 687975.

[22] Aran D, Hu Z, Butte AJ. xCell: digitally portraying the tissue cellular heterogeneity landscape. Genome Biology. 2017; 18: 220.

[23] Newman AM, Liu CL, Green MR, Gentles AJ, Feng W, Xu Y, *et al*. Robust enumeration of cell subsets from tissue expression profiles. Nature Methods. 2015; 12: 453–457.

[24] Becht E, Giraldo NA, Lacroix L, Buttard B, Elarouci N, Petitprez F, *et al*. Estimating the population abundance of tissue-infiltrating immune and stromal cell populations using gene expression. Genome Biology. 2016; 17: 218.

[25] Li T, Fan J, Wang B, Traugh N, Chen Q, Liu JS, *et al*. TIMER: A Web Server for Comprehensive Analysis of Tumor-Infiltrating Immune Cells. Cancer Research. 2017; 77: e108–e110.

[26] Li T, Fu J, Zeng Z, Cohen D, Li J, Chen Q, *et al*. TIMER2.0 for analysis of tumor-infiltrating immune cells. Nucleic Acids Research. 2020; 48: W509–W514.

[27] Jiang P, Lee W, Li X, Johnson C, Liu JS, Brown M, *et al*. Genome-Scale Signatures of Gene Interaction from Compound Screens Predict Clinical Efficacy of Targeted Cancer Therapies. Cell Systems. 2018; 6: 343–354.e5.

[28] Louis DN, Giannini C, Capper D, Paulus W, Figarella-Branger D, Lopes MB, *et al*. cIMPACT-NOW update 2: diagnostic clarifications for diffuse midline glioma, H3 K27M-mutant and diffuse astrocytoma/anaplastic astrocytoma, IDH-mutant. Acta Neuropathologica. 2018; 135: 639–642.

[29] Brat DJ, Aldape K, Colman H, Holland EC, Louis DN, Jenkins RB, *et al*. cIMPACT-NOW update 3: recommended diagnostic criteria for "Diffuse astrocytic glioma, IDH-wildtype, with molecular features of glioblastoma, WHO grade IV". Acta Neuropathologica. 2018; 136: 805–810.

[30] Bell EH, Zhang P, Fisher BJ, Macdonald DR, McElroy JP, Lesser GJ, *et al*. Association of MGMT Promoter Methylation Status With Survival Outcomes in Patients With High-Risk Glioma Treated With Radiotherapy and Temozolomide: An Analysis From the NRG Oncology/RTOG 0424 Trial. JAMA Oncology. 2018; 4: 1405–1409.

[31] Li J, Sun X, He P, Liu WQ, Zou YB, Wang Q, *et al*. Ubiquitin-like modifier activating enzyme 2 promotes cell migration and invasion through Wnt/β-catenin signaling in gastric cancer. World Journal of Gastroenterology. 2018; 24: 4773–4786.

[32] Grabowski MM, Sankey EW, Ryan KJ, Chongsathidkiet P, Lorrey SJ, Wilkinson DS, *et al*. Immune suppression in gliomas. Journal of Neuro-oncology. 2021; 151: 3–12.

[33] Lee EQ. Immune checkpoint inhibitors in GBM. Journal of Neuro-oncology. 2021; 155: 1–11.

[34] Reardon DA, Brandes AA, Omuro A, Mulholland P, Lim M, Wick A, *et al*. Effect of Nivolumab vs Bevacizumab in Patients With Recurrent Glioblastoma: The CheckMate 143 Phase

3 Randomized Clinical Trial. JAMA Oncology. 2020; 6: 1003–1010.

[35] Lim M, Weller M, Idbaih A, Steinbach J, Finocchiaro G, Raval RR, *et al*. Phase III trial of chemoradiotherapy with temozolomide plus nivolumab or placebo for newly diagnosed glioblastoma with methylated MGMT promoter. Neuro-oncology. 2022; 24: 1935–1949.

[36] Nayak L, Molinaro AM, Peters K, Clarke JL, Jordan JT, de Groot J, *et al*. Randomized Phase II and Biomarker Study of Pembrolizumab plus Bevacizumab versus Pembrolizumab Alone for Patients with Recurrent Glioblastoma. Clinical Cancer Research: an Official Journal of the American Association for Cancer Research. 2021; 27: 1048–1057.

[37] Brown NF, Ng SM, Brooks C, Coutts T, Holmes J, Roberts C, *et al*. A phase II open label, randomised study of ipilimumab with temozolomide versus temozolomide alone after surgery and chemoradiotherapy in patients with recently diagnosed glioblastoma: the Ipi-Glio trial protocol. BMC Cancer. 2020; 20: 198.

[38] Mahajan S, Schmidt MHH, Schumann U. The Glioma Immune Landscape: A Double-Edged Sword for Treatment Regimens. Cancers. 2023; 15: 2024.

[39] Segura-Collar B, Hiller-Vallina S, de Dios O, Caamaño-Moreno M, Mondejar-Ruescas L, Sepulveda-Sanchez JM, *et al*. Advanced immunotherapies for glioblastoma: tumor neoantigen vaccines in combination with immunomodulators. Acta Neuropathologica Communications. 2023; 11: 79.

[40] Schakelaar MY, Monnikhof M, Crnko S, Pijnappel EW, Meeldijk J, Ten Broeke T, *et al*. Cellular immunotherapy for medulloblastoma. Neuro-oncology. 2023; 25: 617–627.

[41] Li J, Sun Y, Zhao X, Ma Y, Xie Y, Liu S, *et al*. Radiation induces IRAK1 expression to promote radioresistance by suppressing autophagic cell death via decreasing the ubiquitination of PRDX1 in glioma cells. Cell Death & Disease. 2023; 14: 259.

[42] Saito K, Kagawa W, Suzuki T, Suzuki H, Yokoyama S, Saitoh H, *et al*. The putative nuclear localization signal of the human RAD52 protein is a potential sumoylation site. Journal of Biochemistry. 2010; 147: 833–842.

[43] Jiang Z, Fan Q, Zhang Z, Zou Y, Cai R, Wang Q, *et al*. SENP1 deficiency promotes ER stress-induced apoptosis by increasing XBP1 SUMOylation. Cell Cycle (Georgetown, Tex.). 2012; 11: 1118–1122.

[44] Xu Y, Li J, Zuo Y, Deng J, Wang LS, Chen GQ. SUMO-specific protease 1 regulates the in vitro and in vivo growth of colon cancer cells with the upregulated expression of CDK inhibitors. Cancer Letters. 2011; 309: 78–84.

[45] Zhou F, Dai A, Jiang Y, Tan X, Zhang X. SENP 1 enhances hypoxia induced proliferation of rat pulmonary artery smooth muscle cells by regulating hypoxia inducible factor 1α. Molecular Medicine Reports. 2016; 13: 3482–3490.

[46] Zhou L, Zheng L, Hu K, Wang X, Zhang R, Zou Y, *et al*. SUMOylation stabilizes hSSB1 and enhances the recruitment of NBS1 to DNA damage sites. Signal Transduction and Targeted Therapy. 2020; 5: 80.

[47] Wu YJ, Huang ST, Chang YH, Lin SY, Lin WL, Chen YJ, *et al*. SUMO-Activating Enzyme Subunit 1 Is Associated with Poor Prognosis, Tumor Progression, and Radio-Resistance in Colorectal Cancer. Current Issues in Molecular Biology. 2023; 45: 8013–8026.

[48] Zhu X, Chen D, Sun Y, Yang S, Wang W, Liu B, *et al*. LncRNA WEE2-AS1 is a diagnostic biomarker that predicts poor prognoses in patients with glioma. BMC Cancer. 2023; 23: 120.

[49] Zhao M, Li X, Chen Y, Wang S. MD2 Is a Potential Biomarker Associated with Immune Cell Infiltration in Gliomas. Frontiers in Oncology. 2022; 12: 854598.

[50] Montemurro N, Pahwa B, Tayal A, Shukla A, De Jesus Encarnacion M, Ramirez I, *et al*. Macrophages in Recurrent Glioblastoma as a Prognostic Factor in the Synergistic System of the Tumor Microenvironment. Neurology International. 2023; 15: 595–608.

[51] Beylerli O, Encarnacion Ramirez MDJ, Shumadalova A, Ilyasova T, Zemlyanskiy M, Beilerli A, *et al*. Cell-Free miRNAs as Non-Invasive Biomarkers in Brain Tumors. Diagnostics (Basel, Switzerland). 2023; 13: 2888.